Polymer 97 (2016) 131–137

Contents lists available at ScienceDirect

Polymer

journal homepage: www.elsevier.com/locate/polymer

An efficient approach to the preparation of polyethylene magnetic nanocomposites

Muhammad Nisar [a], Carlos Bergmann [b], Julian Geshev [c], Raúl Quijada [d], Griselda Barrera Galland [a, *]

[a] Instituto de Química, Universidade Federal do Rio Grande do Sul, Av. Bento Gonçalves, 9500, 91501-970 Porto Alegre, Brazil
[b] Laboratório de Materiais Cerâmicos, Departamento de Materiais, Universidade Federal do Rio Grande do Sul, Porto Alegre, Brazil
[c] Instituto de Física, Universidade Federal do Rio Grande do Sul, Porto Alegre, Brazil
[d] Departamento de Ingeniería Química y Biotecnología, Facultad de Ciencias Físicas y Matemáticas, Universidad de Chile, Santiago, Chile

ARTICLE INFO

Article history:
Received 10 March 2016
Received in revised form
9 May 2016
Accepted 10 May 2016
Available online 11 May 2016

Keywords:
Polyethylene
Carbon nanotubes
Magnetic nanocomposites

ABSTRACT

In the present work, a new method is developed for the preparation of polyethylene magnetic nanocomposites by *in situ* polymerization. Carbon nanotubes (CNTs), synthesized by the chemical vapor deposition method using ferrocene as the precursor and catalyst and silica (SiO_2) as the support, were used as fillers and compared with a commercial CNT. The synthesized nanofillers had iron magnetic particles encapsulated in CNTs. The fillers were well dispersed into the polyethylene matrix, as evidenced by scanning electron microscopy (SEM) and transmission electron microscopy (TEM) micrographs. Even for a very low filler concentration of 0.9 wt%, the presence of magnetic nanoparticles changed the diamagnetic nature of the polymer matrix to a ferromagnetic one. The thermal properties showed that the polymeric matrix did not change their properties significantly.

1. Introduction

Polymer matrices filled with inorganic nanoparticles (NPs) with improved mechanical properties, thermal stability, flam retardancy, chemical resistance, and electrical conductivity represent an area of growing scientific interest [1,2]. Carbon nanotubes (CNTs) were first reported in 1991 by Iijima [3]. Apart from its status as a conventional filler, the attractive mechanical thermal and electrical properties, high flexibility [4], and low mass density [5] of CNTs have gained attention in various fields of research, such as chemistry, physics, material science, and electrical engineering [6–9]. Treacy et al. [10] found that the average Young's modulus of isolated CNT reaches 1.8 TPa. Theoretical and experimental results have confirmed that single-wall CNTs demonstrate a high tensile modulus and tensile strength [11,12]. Wong *et al.* [13] determined the mechanical properties of multi-walled carbon nanotubes (MWNTs) using atomic force microscopy; these researchers established that they can be characterized by a very high toughness. In 1994, Ajayan et al. [14] reported on polymer nanocomposites using CNTs as filler for the first time. Earlier works used carbon black, silica, clays, and carbon nanofibers (CNFs) as fillers. In electromagnetic induction shielding, nanotubes have significant advantage over the conventional nanofillers used in the manufacture of multifunctional polymer composites [7,15].

In recent years, the use of CNTs as a reinforcing material for polymer has received enormous attention [6,16–18]. However, the dispersion of CNTs in the polymer matrix has to be taken into consideration to transfer the exceptional properties of CNTs to a polymeric material. The homogenous dispersion of CNTs throughout a polymer matrix is difficult to achieve because there must be considerable interaction between the polymer chain and the CNTs. Their small size and large surface area, as well as the delocalization of π electron subject the CNTs to van der Waals forces, all enhance aggregation [19–21]. An important issue is the compatibility of non-polar polymer matrices and CNTs to induce strong interaction between a polymer phase and filler, and consequently, to produce the efficient reinforcement of composites. In contrast, in the case of polar matrices, the problem seems easier to overcome; Zhang et al. [22,23] presented good results using nylon-6. Applying the same route, however, Tang et al. [24] and Bhattacharyya et al. [25] were unable to achieve significant dispersion of CNTs in polyolefin matrices due to the low compatibility of their apolar nature, which results in CNT aggregation. A number of

* Corresponding author.

http://dx.doi.org/10.1016/j.polymer.2016.05.029
0032-3861/

methods in the literature have been reported for the dispersion of CNTs in polymer matrices, for example, solution blending, melt mixing, and *in situ* polymerization [13,26–28]. This last method, where the filler is introduced during the polymerization reaction, is one of the most attractive routes to produce nanocomposites. This technique is known to be more effective in obtaining homogeneous dispersions of filler as compared to other conventional mechanical melt mixings.

Both academic and industrial researchers are extremely interested in exploring multifunctional magnetic polymer nanocomposites. These materials can potentially be used in many fields, for example, as microwave absorber, magnetic recording materials, energy storage devices, magnetic sensors, and for drug delivery [29]. The physical or chemical dispersion of magnetic elements, such as iron [30,31], cobalt [32,33], and nickel [34,35], into a polymer matrix can be carried out through the following approaches: *in situ* polymerization [36,37], surface-initiated polymerization [38,39], solution blending [40,41], ball milling [42], surface wetting [43], ion exchange [44], and melt blending [45,29]. Iron is one of the most traditionally used magnetic elements [46], and the magnetic performance of iron NPs has recently attracted a great deal of attention. The synthesis routes of iron NPs from soluble precursors in solutions include chemical reduction [47,48] and thermal [49,50] or sonochemical decomposition [51]. Similar to the conventional CNTs, iron NPs also tend to aggregate due to van der Waals forces, high surface energy, and large specific area. To efficiently disperse and control the particle growth, dispersants or surfactants are added during the fabrication of NPs in solution [50,51]. For instance, Burke et al. [50] carried out several sophisticated steps to produce polymer-Fe nanocomposites in the presence of ammonia and polymer (polyisobutylene, polyethylene, and polystyrene) grated with tetraethylenepentamine from the decomposition of $Fe(CO)_5$. Similarly, Tannenbaum et al. [52] reported an iron oxide nanocluster (γ-Fe_2O_3) from the thermal decomposition of $Fe(CO)_5$, where the synthesis process also involves complicated steps.

One of the most significant disadvantages of iron NPs is their easy oxidation. A recent study showed that the encapsulation of magnetic nanoparticles in CNTs could solve this problem [53,54]. Ferrocene [$Fe(C_2H_5)_2$] is a feasible organometallic compound used as an alternative to produce CNTs that does not require high temperature and acts both as a precursor and a catalyst of synthesis [55,56]. More recently, Osorio et al. [57,58] optimized the synthesis of CNTs with ferrocene using silica nanopowders with different surface areas as a substrate. The results showed that it is possible to control the final magnetic properties, that is, the composition of iron-containing phases in CNTs, by varying the temperature and dwell time of synthesis.

Our research group have been extensively working on synthesizing polyolefin nanocomposites using *in situ* polymerization. Recently, we prepared polyethylene–graphite nanosheet (PE-GNS) and isotactic polypropylene–graphite nanosheet (iPP-GNS) nanocomposites and obtained homogenous dispersions of the filler in the polymer matrix [59–64]. The present work aims to obtain nanocomposites of polyethylene iron encapsulated in carbon nanotubes (PE-CNTFe) through *in situ* polymerization using metallocene [$(nBuCp)_2ZrCl_2$] as a catalyst and methylaluminoxane (MAO) as a *co*-catalyst. The characterization of the nanocomposites and their magnetic properties were also studied.

2. Experimental

2.1. Materials

All compounds sensitive to air and moisture (*i.e.*, the catalyst and co-catalyst) were manipulated under deoxygenated dry argon using the standard Schlenk and vacuum line techniques. CNTs were acquired from BAYER®. Toluene was distilled with metallic sodium and benzophenone. MAO (Witco, 10 wt% Al solution in toluene) and metallocene catalyst bis(*n*-butyl)cyclopentadienylzirconium dichloride (n-$BuCp)_2ZrCl_2$ (Sigma Aldrich) were used as received.

2.2. Carbon nanotube synthesis

Two types of CNTs were used in this work: Commercial CNTs were acquired from BAYER®, and synthetic CNTs containing iron were synthesized using the method reported in Refs. 57 and 58. The characterization of the CNT-Fe by TEM can be seen in reference 58 as well as in the Supplementary Data.

2.3. Fabrication of polymer nanocomposites

The CNTs were stirred with 15 wt% of MAO over 30 min in toluene. The polymerization reactions were performed in a 300 mL reactor equipped with mechanical stirring at a controlled temperature. Toluene was used as solvent, MAO as co-catalyst (Al/Zr = 1000) and (n-$BuCp)_2ZrCl_2$ as catalyst (5×10^{-6} mol). All the reactions were carried out at 25 °C with a constant ethylene pressure of 3 bar over 0.5 h. The CNTs that were previously treated with MAO were introduced to the reactor as filler using a changeable quantity under inert atmosphere. The obtained polymer was washed with 10 vol% of HCl in ethanol solution and dried until it reached a constant weight.

2.4. Characterization of polymer nanocomposites

Transmission electron microscopy (TEM) analyses were performed using a JEOL 1011 microscope operating at 120 kV. Samples were prepared *via* the deposition of a solution drop on a copper grid of 300 mesh covered with amorphous carbon. Scanning electron microscopy (SEM) was carried using a Phillips XL30 microscope operating at 20 kV. Samples were prepared by deposition on an aluminum stub and coating with gold.

The molecular weights were obtained with a Waters Alliance GPC 2000 instrument equipped with three Styragel HT-type columns (HT3, HT5, and HT6E). 1,2,4-Trichlorobenzene was used as solvent, with a flow rate of 1 ml/min and a temperature of 135 °C. The columns were calibrated with polystyrene standards.

The magnetic characterization of the CNTs was performed using an EZ9MicroSense vibrating sample magnetometer (VSM) at room temperature with a magnetic field (H) ranging from −20 kOe to +20 kOe. Dynamic mechanical analysis (DMA) were obtained using a DMA analyzer (TA Instruments model Q800). The samples were analyzed in single-cantilever mode at a frequency of 1 Hz and a strain level of 0.1% in the temperature range of −140 °C to 120 °C.

Differential scanning calorimetric (DSC) analyses were performed using a Perkin-Elmer differential calorimeter (model DSC Q20) operating at a heat rate of 10 °C/min and a temperature range from 0 to 180 °C. The melting temperature, T_m, was determined in the second scan, and the degree of crystallinity was calculated from the enthalpy of fusion data obtained from the DSC curves (293 J/g was used for 100% crystalline material). Thermogravimetric analysis (TGA) was performed on a SDT Q600 thermal analyzer Q20 (TA Instruments) at a scanning rate of 20 °C/min from 0 °C to 800 °C.

3. Results and discussion

Polymerizations of ethylene were performed in the presence of commercial CNT and of synthesized iron NPs encapsulated in CNTs (CNT-Fe). The catalytic activities of these reactions are listed in

Table 1
Results of nanocomposites of polyethylene with different amounts of CNTs and CNT-Fe.

Samples	Filler[b] (%)	Polymer (g)	Catalytic activity[a]	T_c (°C)	T_m (°C)	X_c (%)	T_g (°C)	T_{max}
PE	0	7.40	966	113	139	55	−114	487
PE_{CNT}	1.1	6.95	927	115	138	62	−111	490
PE_{CNT}	3.4	6.01	801	115	138	58	–	493
PE_{CNT-Fe}	0.9	8.20	1093	113	141	53	−113	484
PE_{CNT-Fe}	2.5	7.48	998	114	139	55	–	483

[a] KgPE/[Zr] h bar.
[b] CNT or CNT-Fe.

Table 1, along with the polymerization without filler (neat polyethylene). It can be seen that with the treatment using CNTs or CNT-Fe did not deactivate the catalyst, since the activities were almost the same in all the reactions.

Table 1 also shows the thermal properties of the neat polyethylene and its nanocomposites. Neither the crystallinity (X_c) nor the T_m showed significant variation compared with the original polymer. The crystallization temperature (T_c) of the nanocomposites, however, showed a slight increase of 1–2 °C with the addition of a small amount of CNTs (1.1%). In addition, the glass transition temperature, T_g, also increased up to 3 °C with the incorporation of CNTs, which provides evidence for the reinforcement effect of the CNTs. The molecular weight of the neat polymer was significantly high (4.4×10^5 g mol^{-1} with a polydispersity of 1.9), which was also confirmed by the high melting temperature (139 °C). Previous preparations of polyolefin nanocomposites using the same method showed that the nanocomposites maintain the same molecular weight as the neat polymer [61]; in this case, this was also confirmed by the similar T_m. The maximum temperature (T_{max}) of degradation obtained by TGA showed a slight increase with the incorporation of CNTs and a small decrease with the addition of CNT-Fe. The increase in degradation of the nanocomposites in the presence of synthetic filler is considered to be due to the presence of iron in the filler, which acts as a catalyst of degradation. The nanocomposites did not show conductivity, as the amount of the filler was below the electrical percolation threshold.

Fig. 1 gives SEM micrographs of polyethylene/CNT nanocomposites with different loadings of filler. The micrographs show a fibrous morphology, indicating that the CNTs were coated by polyethylene. This type of morphology is mainly attributed to the low-temperature polymerization; the fibrous morphology is more prominent as the loading of CNTs with iron increases. Bahuleyan et al. [65] reported the absence of fibrous morphology at high polymerization temperatures, such 60 °C. The nanotubes seem to have a uniform dispersion in the polymer matrix.

A TEM morphological assessment of the prepared nanocomposites was performed. Fig. 2 shows representative micrographs of nanocomposites with similar magnifications. The dispersion quality of the filler in the polymer matrix was very good, and all CNTs showed homogenous dispersion, as no aggregation was observed. The TEM images confirm that CNTs and the polymer matrix form close interfaces without gaps.

4. Magnetic properties

The room temperature magnetization hysteresis loops of the CNT-Fe powder, PE-CNT-Fe and PE-CNT samples are plotted in Fig. 3. The magnetization curve of the PE-CNT sample (not shown) presented only diamagnetic characteristics with no hysteresis, evidencing absence of magnetic material in the CNTs. The

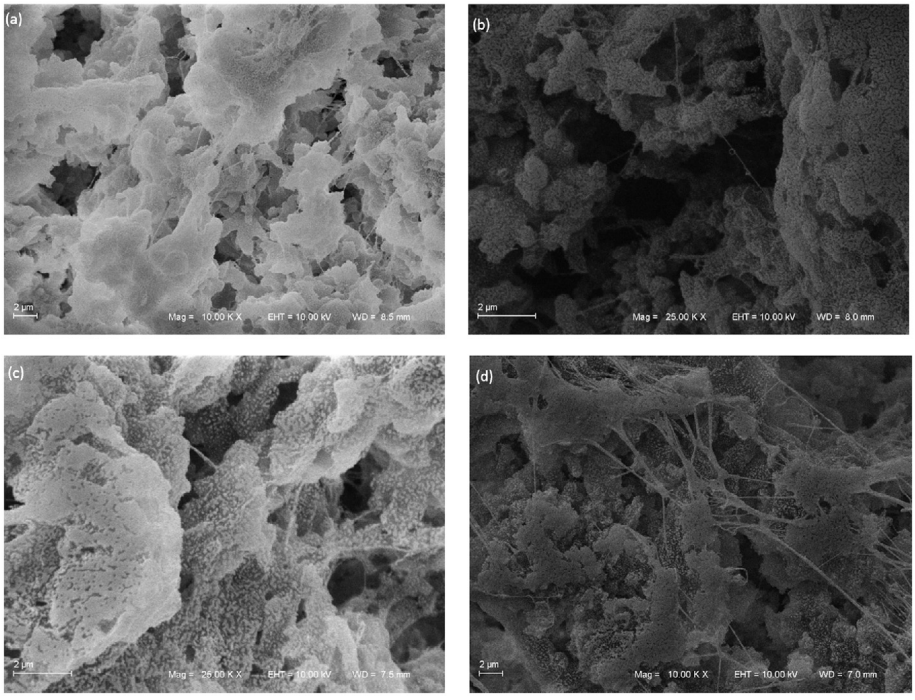

Fig. 1. SEM images of nanocomposites: (a) 1.1% and (b) 3.4% CNTs in PE; (c) 0.9% and (d) 2.5% CNT-Fe in PE.

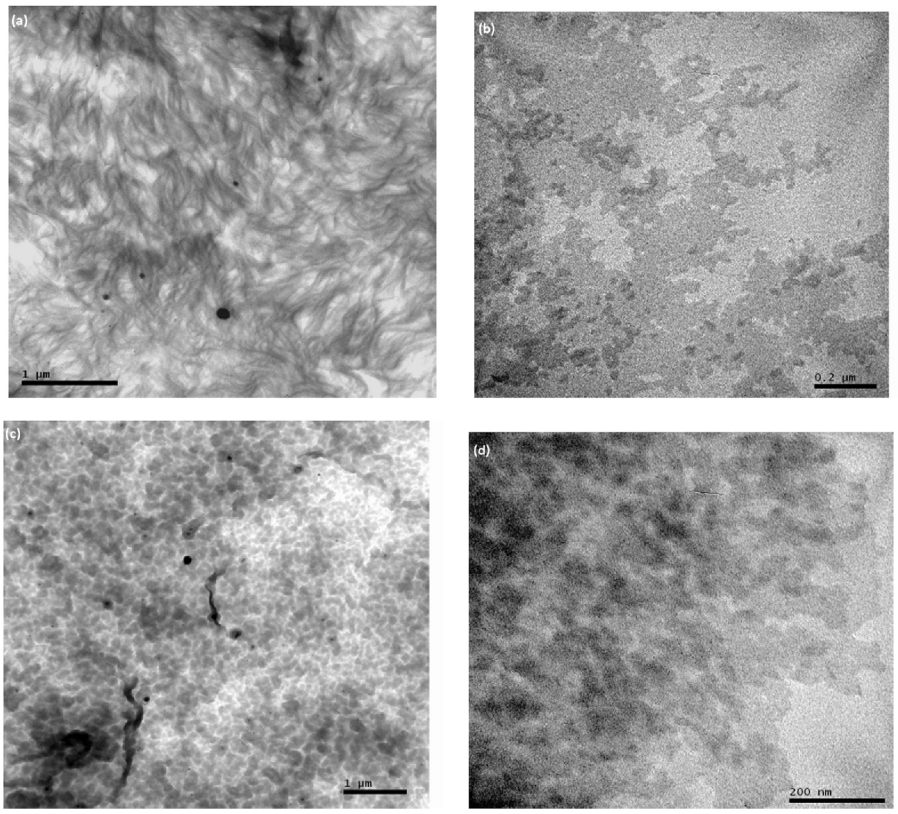

Fig. 2. TEM images of nanocomposites: (a) and (b) 2.5% CNTs-Fe in PE; (c) and (d) 0.9% CNTs-Fe in PE.

hysteresis loops for the PE-CNT-Fe 0.9 and 2.5 wt% samples turned out to be extremely similar, showing almost identical values of remnant magnetization/saturation magnetization (M_R/M_S) and coercivity (H_C), with the latter equal to ~1000 Oe. Table 2 gives the respective H_C and normalized (to the saturation magnetization value, M_S) remnant magnetization, M_R, of the nanocomposites. Recently, Riquelme et al. [29] reported on polypropylene magnetic nanocomposites by melt mixing, where they also used iron encapsulated in CNTs. They obtained a coercivity value of 500–550 Oe for 2–6% of nanotubes, which is half the value we obtained for 0.9–2.5% of filler. Similarly, Santos et al. [66] obtained coercivity of 275 and 250 Oe for polyurethanes, PU/3 and PU/10 wt % of Fe_3O_4 synthetic talc, that is, values approximately four times lower than ours. He *et al.* [67] reported a decrease from 193 to 9 Oe in H_C, with an increase from 5 to 20 wt% of magnetic particles in a high density polyethylene (HDPE) matrix. This can be ascribed to a decrease in inter-particle distance resulting in stronger (negative, demagnetizing) dipolar interactions, which tend to stabilize the demagnetized state with low remnant and coercivity values. In our case, H_C decreased slightly (from 1060 to ~1000 Oe) when the magnetic constituent was increased from 0.9 to 2.5%, which we attribute to the fact that the mean inter-particle distance is practically the same in both samples owing to the low amount of magnetic constituent (≤2.5%). This indicates a rather uniform dispersion of CNTs in the polymer matrix confirmed by the SEM and TEM analyses.

The above statement is strongly supported by additional

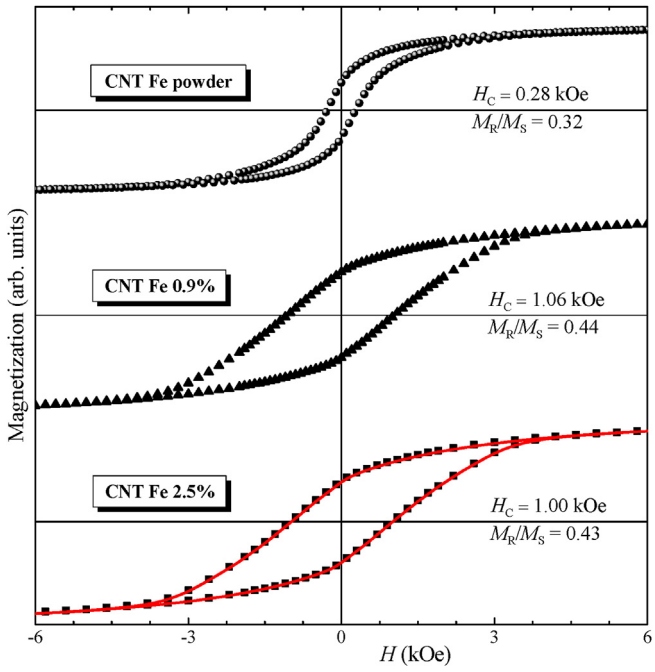

Fig. 3. Room-temperature hysteresis loops of (a) CNT-Fe powder, (b) CNT-Fe 0.9% in PE, and (c) CNT-Fe 2.5% in PE. The solid line in the bottom panel corresponds to a measurement on the same sample but performed approximately 6 months after the first loop trace (square symbols); during this period of time the sample was kept in air.

Table 2
H_C and M_R/M_S values of the nanocomposites extracted from the room-temperature VSM measurements.

Sample	H_C (Oe)	M_R/M_S
PE-CNT 3.4%	0	0
CNT-Fe	280(±10)	0.32
PE-CNT-Fe 0.9%	1060(±10)	0.44
PE-CNT-Fe 2.5%	1000(±10)	0.43

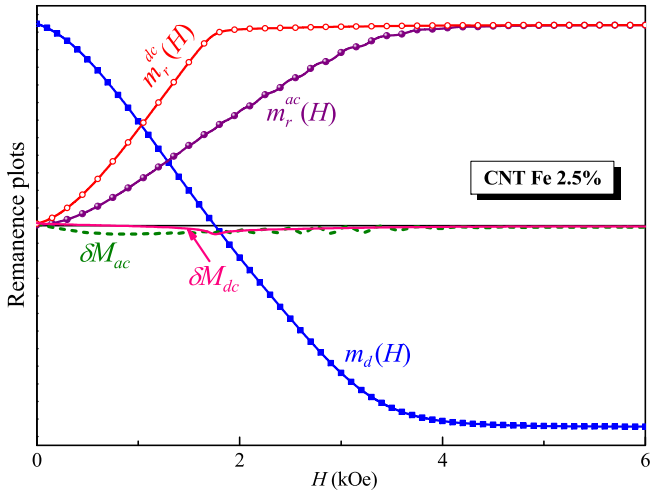

Fig. 4. Room-temperature remnant magnetization curves (both ac and dc types of demagnetization were used) and the corresponding δM plots for the CNT-Fe 2.5% PE nanocomposite.

interaction-effect measurements performed on the CNT-Fe 2.5% PE sample. We employed the so-called remanence-plots technique [68,69], which exploits relationships between the isothermal remanence magnetization [IRM or $m_r(H)$] and the dc demagnetization [DCD, or $m_d(H)$] curves, which are very sensitive to small changes in the remnant state produced by magnetic interactions; details of the method can be found elsewhere [70,71]. The value of the maximum field we used was sufficient for effective magnetic saturation, thereby avoiding minor-loop effects [72–76]. The $m_r(H)$ (measured on either an ac or dc demagnetized sample) and the $m_d(H)$ curves, together with the corresponding δM plots [77,78], are given in Fig. 4. Both δM plots confirm that the inter-particle interactions were demagnetizing and extremely weak.

Fig. 5 shows magnetic measurements on CNT-Fe in a powder form, being the interval between the first and the second loop traces of approximately 6 months, during which the sample was kept in air. One notes that the hysteresis loops are practically

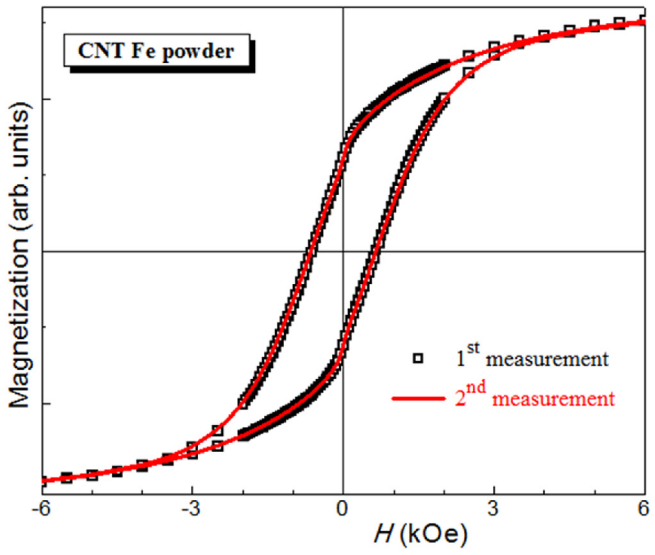

Fig. 5. Two room-temperature hysteresis loops traced on powdered CNT-Fe. The interval between the first and the second measurements is approximately 6 months, during which the powder was kept in air.

indistinguishable (the same holds for the sample CNT-Fe 2.5% in PE, see the bottom panel of Fig. 3), which strongly indicates that the encapsulation of the iron nanoparticles in CNT protects them from oxidation and aggregation.

5. Conclusions

A new magnetic nanocomposite of polyethylene/CNT-Fe was obtained through the *in situ* polymerization of ethylene using $(nBuCp)_2ZrCl_2$/MAO as a catalyst system. The rather high coercivity values (~1000 Oe) obtained here should be attributed to two techniques we employed, namely: 1) the encapsulation of Fe in CNT, which protected the iron NPs from oxidation and aggregation; and 2) the *in situ* polymerization method, that allows a uniform dispersion of CNTs in the polymer matrix and avoids dipolar interactions, which tend to stabilize the demagnetized state. This new material, which maintains all of the excellent properties of polyethylene and adds a magnetic characteristic, has the potential to be used in a variety of applications where a flexible magnetic material with good processability could be required.

Acknowledgments

The authors are grateful to the TWAS-CNPQ for the fellowship to Muhammad Nisar, the CNPq for the special visiting research fellowship to Professor Raúl Quijada, and CNPq grant 302902/2013-9. Professor Raúl Quijada acknowledges the Millennium Nucleus of Chemical Processes and Catalysis (CPC), grant number NC120082. We also thank CME and LRNANO from UFRGS for the microscopy analysis.

Appendix A. Supplementary data

Supplementary data related to this article can be found at http://dx.doi.org/10.1016/j.polymer.2016.05.029.

References

[1] J. Jancar, J.F. Douglas, F.W. Starr, S.K. Kumar, P. Cassagnau, A.J. Lesser, S.S. Sternstein, M. Buehler, Current issues in research on structural-property relationship in polymer nanocomposites, Polymer 51 (2010) 3321–3343.
[2] I.Y. Jeon, J.B. Baek, Nanocomposites derived from polymers and inorganic nanoparticles, Materials 3 (2010) 3654–3674.
[3] S. Iijima, Helical Microtubules of Graphitic Carbon, vol. 354, Nature, London, 1991, pp. 56–58.
[4] C.A. Cooper, R.J. Young, M. Halasll, Investigation into the deformation of carbon nanotubes and their composites through the use of Raman Spectroscopy, Compos. Part A 32 A (2001) 401–411.
[5] G. Gao, T. Cagin, W.A. Goddard III, Energetics, structure, mechanical and vibrational properties of single walled carbon nanotubes, Nanotechnology 9 (1998) 184–191.
[6] R.H. Baughman, A.A. Zakhivov, W.A. De Heer, Carbon nanotubes the route toward applications, Science 297 (2002) 787–792.
[7] P.M. Ajayan, Nanotubes from carbon, Chem. Rev. 99 (1999) 1787–1800.
[8] C.A. Grimes, C. Mungle, D. Kouzoudis, S. Fang, P.C. Eklund, The 500 MHz to 5.50 GHz complex permittivity spectra of single-wall carbon nanotube-loaded polymer composites, Chem. Phys. Lett. 319 (2000) 460–464.
[9] B.S. File, B.M. Mayeaux, Carbon nanotubes, Adv. Matter. Process 156 (1999) 47–49.
[10] M.M.J. Treacy, T.W. Ebbesen, J.M. Gibson, Exceptionally high Young's modulus observed for individual carbon nanotubes, Nature 381 (1996) 678–680.
[11] T. Uchida, S. Kumar, Single wall carbon nanotube dispersion and exfoliation in polymers, J. Appl. Polym. Sci. 98 (2005) 985–989.
[12] A. De Heer Walt, Nanotubes and the pursuit of applications, MRS. Bull. 29 (2004) 281–285.
[13] E.W. Wong, P.E. Sheehan, C.M. Lieber, Nanobeam mechanics: elasticity, strength and toughness of nanorods and nanotubes, Science 277 (1997) 1971–1975.
[14] P.M. Ajayan, O. Stephan, C. Colliex, D. Trauth, Aligned carbon nanotubes arrays formed by cutting a polymer resin-nanotube composites, Science 265 (1994) 1212–1214.
[15] M. Moniruzzaman, K.I. Winey, Polymer nanocomposites containing carbon nanotubes, Macromolecules 39 (2006) 5194–5205.

[16] E.T. Thostenton, Z. Ren, T.W. Chou, Advances in the *science* and *technology* of carbon nanotubes and their composites: a review, Compos. Sci. Technol. 61 (2001) 1899–1912.
[17] R. Andrews, M.C. Weisenberger, Carbon nanotube polymer composites, Curr. Opin. Solid State Mater. Sci. 8 (2004) 31–37.
[18] A.K.T. Lau, D. Hui, Strength and durability performance of concrete axially loaded members confined with AFRP composite sheets, Compos. Part B 33 (2002) 263–277.
[19] S. Bredeau, S. Peeterbroeck, D. Bonduel, M. Alexandre, P. Dubois, From carbon nanotube coatings to high-performance polymer nanocomposites, Polym. Int. 57 (2008) 547–553.
[20] P. Ajayan, in: H.S. Nalwa (Ed.), Handbook of Nanostructured Materials and Nanotechnology, 5, Academic Press, New York, 2000, pp. 501–575.
[21] C. Wang, Z. Guo, S. Fu, W. Wu, D. Zhu, Polymers containing fullerene or carbon nanotube structures, Prog. Polym. Sci. 29 (2004) 1079–1141.
[22] W.D. Zhang, L. Shen, I.Y. Phang, T. Liu, Carbon nanotubes reinforced nylon-6 composite prepared by simple melt-compounding, Macromolecules 37 (2004) 256–259.
[23] T. Liu, I.Y. Phang, L. Shen, S.Y. Chows, W.D. Zhang, Morphology and mechanical. properties of multiwalled carbon nanotubes. Reinforced Nylon-6 composites, Macromolecules 37 (2004) 7214–7222.
[24] W. Tang, M.H. Santare, S.G. Advani, Melt processing and mechanical property characterization of multi-walled carbon nanotube/high density polyethylene (MWNT/HDPE) composite films, Carbon 41 (2003) 2779–2785.
[25] A.R. Bhattacharyya, T.V. Sreekumer, T. Liu, S. Kumar, L.M. Ericson, R.H. Hauge, R.E. Smalley, Crystallization and orientation studies in polypropylene/single wall carbon nanotube composite, Polymer 44 (2003) 2373–2377.
[26] X.L. Xie, Y.W. Mai, X.P. Zhou, Dispersion and alignment of carbon nanotubes in polymer matrix: a review, Mater. Sci. Eng. 49 (2005) 89–112.
[27] L. Ashabi, S.H. Jafari, H.A. Khonakdar, B. Baghaei, Morphological, rheological and thermal studies in melt processed compatibilized PA6/ABS/clay nanocomposites, J. Polym. Res. 18 (2011) 197–205.
[28] K. Saeed, S.Y. Park, Preparation and characterization of multiwalled carbon nanotubes/polyacrylonitrile nanofibers, J. Polym. Res. 17 (2010) 535–540.
[29] J. Riquelme, C. Garzón, B. Bergmann, J. Geshev, R. Quijada, Development of multifunctional polymer nanocomposites with carbon-based hybrid nanostructures synthesized from ferrocene, Eur. Polym. J. 75 (2016) 200–209.
[30] S.N. Khanna, S. Linderoth, Magnetic behavior of clusters of ferromagnetic transition metals, Phys. Rev. Lett. 67 (6) (1991) 742–745.
[31] D. Farrell, S.A. Majetich, J.P. Wilcoxon, Preparation and characterization of monodisperse Fe nanoparticles, J. Phys. Chem. B 107 (2003) 11022–11103.
[32] X. Lin, C. Sorensen, K. Klabunde, G.C. Hadjipanayis, Temperature dependence of morphology and magnetic properties of cobalt nanoparticles prepared by an inverse micelle technique, Langmuir 14 (1998) 7140–7146.
[33] C. Petit, A. Taleb, M. Pileni, Cobalt nanosized particles organized in a 2D superlattice: synthesis, characterization, and magnetic properties, J. Phys. Chem. B 103 (1999) 1805–1810.
[34] S. Apsel, J. Emmert, J. Deng, L. Bloomfield, Surface-Enhanced magnetism in nickel clusters, Phys. Rev. Lett. 76 (1996) 1441–1444.
[35] T.O. Ely, C. Amiens, B. Chaudret, E. Snoeck, M. Verelst, M. Respaud, Synthesis of nickel nanoparticles. influence of aggregation induced by modification of poly(vinylpyrrolidone) chain length on their magnetic properties, Chem. Mater. 11 (1999) 526–529.
[36] T.H. Hsieh, K.S. Ho, X. Bi, Y.K. Han, Z.L. Chen, C.H. Hsu, Synthesis and electromagnetic properties of polyaniline-coated silica/maghemite nanoparticles, Eur. Polym. J. 45 (2009) 613–620.
[37] H. Nathani, R. Misra, Surface effects on the magnetic behavior of nanocrystalline nickel ferrites and nickel ferrite-polymer nanocomposites, Mater. Sci. Eng. B 113 (2004) 228–235.
[38] J. Zhu, S. Wei, L. Zhang, Y. Mao, J. Ryu, A.B. Karki, Polyaniline-tungsten oxide metacomposites with tunable electronic properties, J. Mater. Chem. 21 (2011) 342–348.
[39] J. Zhu, S. Wei, L. Zhang, Y. Mao, J. Ryu, N. Haldolaarachchige, Electrical and dielectric properties of polyaniline–Al_2O_3 nanocomposites derived from various Al_2O_3 nanostructures, J. Mater. Chem. 21 (2011) 3952–3959.
[40] J. Zhu, S. Wei, D. Rutman, N. Haldolaarachchige, D.P. Young, Z. Guo, Magnetic polyacrylonitrile-Fe@FeO nanocomposite fibers – electrospinning, stabilization and carbonization, Polymer 52 (2011) 2947–2955.
[41] X. Chen, S. Wei, C. Gunesoglu, J. Zhu, C.S. Southworth, L. Sun, Electrospun magnetic fibrillar polystyrene nanocomposites reinforced with nickel nanoparticles, Macromol. Chem. Phys. 211 (2010) 1775–1783.
[42] A. Ohlan, K. Singh, A. Chandra, S.K. Dhawan, Microwave absorption behavior of core-shell structured poly (3,4-ethylenedioxy thiophene)-barium ferrite nanocomposites, ACS Appl. Mater. Inter 2 (2010) 927–933.
[43] J. Zhu, S. Wei, J. Ryu, L. Sun, Z. Luo, Z. Guo, Magnetic epoxy resin nanocomposites reinforced with core-shell structured Fe@FeO nanoparticles: fabrication and property analysis, ACS Appl. Mater. Inter 2 (2010) 2100–2107.
[44] S. Mu, D. Wu, Y. Wang, Z. Wu, X. Yang, W. Yang, Fabrication of nickel oxide nanocomposite layer on a flexible polyimide substrate via ion exchange technique, ACS Appl. Mater. Inter 2 (2009) 111–118.
[45] J.L. Wilson, P. Poddar, N.A. Frey, H. Srikanth, K. Mohomed, J.P. Harmon, S. Kotha, J. Wachsmuth, Synthesis and magnetic properties of polymer nanocomposites with embedded iron nanoparticles, J. Appl. Phys. 95 (2004) 1439–1443.
[46] S. Wei, Q. Wang, J. Zhu, L. Sun, H. Lin, Z. Guo, Multifunctional composite core–shell nanoparticles, Nanoscale 3 (2011) 4474–4502.
[47] Z. Guo, L.L. Henry, V. Palshin, E.J. Podlaha, Synthesis of poly (methyl methacrylate) stabilized colloidal zero-valence metallic nanoparticles, J. Mater. Chem. 16 (2006) 1772–1777.
[48] Y. Hou, J. Yu, S. Gao, Solvothermal reduction synthesis and characterization of superparamagnetic magnetite nanoparticles, J. Mater. Chem. 13 (2003) 1983–1987.
[49] J. Zhu, S. Wei, Y. Li, L. Sun, N. Haldolaarachchige, D.P. Young, Surfactant-free synthesized magnetic polypropylene nanocomposites: rheological, electrical, magnetic and thermal properties, Macromolecules 44 (2011) 4382–4391.
[50] N.A.D. Burke, H.D.H. Stöver, F.P. Dawson, Magnetic nanocomposites: preparation and characterization of polymer coated iron nanoparticles, Chem. Mater. 14 (2002) 4752–4761.
[51] S. Wizel, S. Margel, A. Gedanken, The preparation of a polystyrene–iron composite by using ultrasound radiation, Polym. Int. 49 (2000) 445–448.
[52] R. Tannenbaum, M. Zubris, P.E. Goldberg, S. Reich, N. Dan, Polymer-directed nanocluster synthesis: control of particle size and morphology, Macromolecules 38 (2005) 4254–4259.
[53] A. Morelos-Gómez, F. Lopez-Urias, E. Munoz-Sandoval, C.L. Dennis, R.D. Shull, H. Terrones, M. Terrones, Controlling high coercivities of ferromagnetic nanowires encapsulated in carbon nanotubes, J. Mater. Chem. 20 (2010) 5906–5914.
[54] C. He, N. Zhao, C. Shi, J. Li, H. Li, Magnatic properties and transmission electron microscopy studies of Ni nanoparticles encapsulated in carbon nanocages and carbon nanotubes, Mater. Res. Bull. 43 (2008) 2260–2265.
[55] R. Bhatia, V. Prasad, Synthesis of multiwall carbon nanotubes by chemical vapor deposition of ferrocene alone, Solid State Commun. 150 (2010) 311–315.
[56] K.P.S.S. Hembram, G.M. Rao, Structural and surface features of multiwall carbon nanotubes, Appl. Surf. Sci. 257 (2011) 5503–5507.
[57] A.G. Osorio, C.P. Bergmann, Effect of surface area of substrates aiming the optimization of carbon nanotube production from ferrocene, Appl. Surf. Sci. 264 (2013) 794–800.
[58] A.G. Osorio, L.G. Pereira, J.B.M. Cunha da, C.P. Bergmann, Controlling the magnetic response of carbon nanotubes filled with iron-containing material, Mater. Res. Bull. 48 (2013) 4168–4173.
[59] F.C. Fim, J.M. Guterres, N.R.S. Basso, G.B. Galland, Polyethylene/Graphite nanocomposites obtained by *in situ* polymerization, J. Polym. Sci. Part A Polym. Chem. 48 (2010) 692–698.
[60] M.A. Milani, R. Quijada, N.R.S. Basso, A.P. Graebin, G.B. Galland, Influence of the graphite type on the synthesis of polypropylene graphene nanocomposites, J. Polym. Sci. Part A Polym. Chem. 50 (2012) 3598–3605.
[61] M.A. Milani, D. González, R. Quijada, N.R.S. Basso, M.L. Cerrada, D.S. Azambuja, G.B. Galland, Polypropylene/graphene nanosheet nanocomposites by *in situ* polymerization: synthesis, characterization and fundamental properties, Compos. Sci. Technol. 84 (2013) 1–7.
[62] F.C. Fim, N.R.S. Basso, A.P. Graebin, D.S. Azambuja, G.B. Galland, Thermal, electrical, and mechanical properties of polyethylene-graphene nanocomposites obtained by in situ polymerization, J. Appl. Polym. Sci. 128 (2013) 2630–2637.
[63] M.A. Milani, D. González, R. Quijada, R. Benavente, J. Arranz-Andrés, G.B. Galland, Synthesis, characterization and properties of poly(propylene-1-octene)/graphite nanosheet nanocomposites obtained by *in situ* polymerization, Polymer 65 (2015) 134–142.
[64] G. Pavoski, T. Maraschin, M.A. Milani, D.S. Azambuja, R. Quijada, C.M. Moura, N.R.S. Basso, G.B. Griselda, Polyethylene/reduced graphite oxide nanocomposites with improved morphology and conductivity, Polymer 81 (2015) 79–86.
[65] B.K. Bahuleyan, M.A. Atieh, S.K. De, M.J. Khan, M.A. Al-Hazrthi, Easy one-pot method to control the morphology of polyethylene/carbon nanotube nanocomposites using metallocene catalysts, J. Polym. Res. 19 (2012) 9744.
[66] L.M.D. Santos, R. Ligabue, A. Dumas, C.L. Roux, P. Micoud, J.F. Meunier, F. Martin, S. Einloft, New magnetic nanocomposites: Polyurethane/Fe_3O_4-synthetic talc, Eup. Polym. J. 69 (2015) 38–49.
[67] Q. He, T. Yuan, J. Zhu, Z. Luo, N. Haldolaarachchige, L. Sun, A. Khasanov, Y. Li, D.P. Young, S. Wei, Z. Guo, Magnetic high density polyethylene nanocomposites reinforced with in-situ synthesized Fe@FeO core-shell nanoparticles, Polymer 53 (2012) 3642–3652.
[68] P.R. Bissel, R.W. Chantrell, G. Tomka, J.E. Knowles, M.P. Sharrock, Remanent magnetisation and demagnetisation measurements on particulate recording media, IEEE Trans. Magn. 25 (1989) 3650–3653.
[69] P.I. Mayo, K. O'Grady, R.W. Chantrell, J.A. Cambridge, I.L. Sanders, T. Yogi, J.K. Howard, Magnetic measurement of interaction effects in CoNiCr and CoPtCr thin film media, J. Magn. Magn. Mater 95 (1991) 109–117.
[70] R. Cichelero, A. Harres, K.D. Sossmeier, J.E. Schmidt, J. Geshev, Magnetic interactions in exchange-coupled yet unbiased IrMn/NiCu bilayers, J. Phys. Condens. Matter 25 (2013) 426001.
[71] A. Harres, R. Cichelero, L.G. Pereira, J.E. Schmidt, J. Geshev, Remanence plots technique extended to exchange bias systems, J. Appl. Phys. 114 (2013) 043902.
[72] L. Klein, Comment on "exchange bias-like phenomenon in SrRuO3" [Appl. Phys. Lett. 88, 102502 (2006)], Appl. Phys. Lett. 89 (2006) 036101.
[73] J. Geshev, Exchange bias and vertical shift in CoFe2O4 nanoparticles, J. Magn. Magn. Mater 320 (2008) 600–602.
[74] J. Geshev, Comment on "Cluster glass induced exchange biaslike effect in the

perovskite cobaltites, Appl. Phys. Lett. 93 (2008) 176101.
[75] J. Geshev, L.G. Pereira, V. Skumryev, Comment on "exchange bias dependence on interface spin alignment in a Ni80Fe20/(Ni,Fe)O thin film, Phys. Rev. Lett. 100 (2008) 039701.
[76] A. Harres, M. Mikhov, V. Skumryev, A.M.H. de Andrade, J.E. Schmidt, J. Geshev, Criteria for saturated magnetization loop, J. Magn. Magn. Mater 402 (2016) 76–82.
[77] P.E. Kelly, K. O'Grady, P.I. Mayo, R.W. Chantrell, Switching mechanisms in cobalt-phosphorus thin film, IEEE Trans. Magn. 25 (1989) 3881–3883.
[78] A.D.C. Viegas, J. Geshev, L.S. Dorneles, J.E. Schmidt, M. Knobel, Correlation between magnetic interactions and giant magnetoresistance in melt-spun $CO_{10}Cu_{90}$ granular alloys, J. Appl. Phys. 82 (1997) 3047–3053.